Inorg. Chem. **2007**, *46*, 10214–10220

One- and Two-Dimensional Silver and Zinc Uranyl Phosphates Containing Bipyridyl Ligands

Yaqin Yu, Wei Zhan, and Thomas E. Albrecht-Schmitt*

Department of Chemistry and Biochemistry and Center for Actinide Science, Auburn University, Auburn, Alabama 36849

Received August 7, 2007

The reaction of AgCN with UO_2, 4,4′-bipy, and phosphoric acid in water at 160 °C under autogeneously generated pressure results in the formation of $[Ag(4,4'\text{-bipy})]_2[(UO_2)_2H_3(PO_4)_3]$ (**AgUP-1**). $Ag(2,2'\text{-bipy})(UO_2)_2(HPO_4)(PO_4)$ (**AgUP-2**) has been prepared from the hydrothermal reaction (at 180 °C) of $KAg(CN)_2$ with $UO_2(C_2H_3O_2)_2{\cdot}2H_2O$ and 2,2′-bipy. $[Zn(2,2'\text{-bipy})]_2[UO_2(HPO_4)_3]$ (**ZnUP-1**) was isolated from the hydrothermal reaction of UO_2, 2,2′-bipyridyl, $Zn(CN)_2$, and H_3PO_4. Single crystal X-ray diffraction experiments reveal that the structure of **AgUP-1** consists of $^2_\infty[(UO_2)_2H_3(PO_4)_3]^{2-}$ expanded autunite-like layers in the [*ac*] plane, separated by $^1_\infty[Ag(4,4'\text{-bipy})]^+$ chains of two-coordinate Ag^+ bridged by 4,4′-bipy. The structure of **AgUP-2** is composed of chains of edge-sharing UO_7 pentagonal bipyramids that are linked by phosphate anions into $^2_\infty[(UO_2)_2(HPO_4)(PO_4)]^{1-}$ sheets with the β-uranophane topology that extend in the [*ab*] plane. Both sides of the sheets are decorated by $[Ag(2,2'\text{-bipy})]^+$ units, where the Ag^+ cations are found in distorted trigonal planar environments. The structure of **ZnUP-1** is 1D and consists of UO_7 pentagonal bipyramids that are connected by phosphate anions that also bind four-coordinate zinc(II) to the periphery of the chains and five-coordinate zinc within the chains. Intense fluorescence from these compounds was observed.

Introduction

Interest in uranium-containing extended structures stems in part from the rich coordination chemistry displayed by uranium(VI) that includes tetragonal, pentagonal, and hexagonal bipyramidal environments.[1] These three units can be used in the construction of diverse architectures that also typically incorporate oxoanions as ligands.[2,3] The formation of extended structures based on uranyl polyhedra can be substantially influenced through the inclusion of organic structure-directing agents, such as organoammonium cations. This strategy has been applied to the synthesis of large classes of fluorides,[4] sulfates,[5] selenates,[6] phosphates,[7] arsenates,[7c] and molybdates.[8] Some of the highlights of these compounds include nanotubular $(C_4H_{12}N)_{14}[(UO_2)_{10}(SeO_4)_{17}(H_2O)]$[6] and chiral frameworks in uranyl molybdates such as $[C_6H_{16}N]_2[(UO_2)_6(MoO_4)_7(H_2O)_2](H_2O)_2$,[8a] $(UO_2)_{0.82}[C_8H_{20}N]_{0.36}[(UO_2)_6(MoO_4)_7(H_2O)_2](H_2O)_n$,[8b] $[C_6H_{14}N_2][(UO_2)_6(MoO_4)_7(H_2O)_2](H_2O)_m$,[8] and $[(C_2H_5)_2NH_2]_2[(UO_2)_4(MoO_4)_5(H_2O)](H_2O)$.[8c] In addition, uranyl polyhedra can be joined into extended structures using organic linkers to yield organic−inorganic

* To whom correspondence should be addressed. E-mail: albreth@auburn.edu.

(1) Burns, P. C.; Ewing, R. C.; Hawthorne, F. C. *Can. Mineral.* **1997**, *35*, 1551.
(2) (a) Burns, P. C.; Miller, M. L.; Ewing, R. C. *Can. Mineral.* **1996**, *34*, 845. (b) Burns, P. C. In *Uranium: Mineralogy, Geochemistry and the Environment*; Burns, P. C., Finch, R., Eds.; Mineralogical Society of America: Washington, DC, 1999; Chapter 1. (c) Burns, P. C. *Mater. Res. Soc. Symp. Proc.* **2004**, *802*, 89.
(3) Burns, P. C. *Can. Mineral.* **2005**, *43*, 1839.
(4) (a) Ok, K. M.; Doran, M. B.; O'Hare, D. *J. Mater. Chem.* **2006**, *16*, 3366. (b) Wang, C.- M.; Liao, C.-H.; Lin, H.-M.; Lii, K.-H. *Inorg. Chem.* **2004**, *43*, 8239. (c) Almond, P. M.; Deakin, L.; Porter, M. J.; Mar, A.; Albrecht-Schmitt, T. E. *Chem. Mater.* **2000**, *12*, 3208. (d) Walker, S. M.; Halasyamani, P. S.; Allen, S.; O'Hare, D. *J. Am. Chem. Soc.* **1999**, *121*, 10513. (e) Francis, R. J.; Halasyamani, P. S.; O'Hare, D. *Angew. Chem.* **1998**, *37*, 2214. (f) Francis, R. J.; Halasyamani, P. S.; O'Hare, D. *Chem. Mater.* **1998**, *10*, 3131.
(5) (a) Doran, M. B.; Cockbain, B. E.; O'Hare, D. *Dalton Trans.* **2005**, *10*, 1774. (b) Doran, M. B.; Norquist, A. J.; O'Hare, D. *Acta Crystallogr.* **2005**, *E61*, m881−m884. (c) Norquist, A. J.; Doran, M. B.; O'Hare, D. *Acta Crystallogr.* **2005**, *E61*, m807−m810. (d) Norquist, A. J.; Doran, M. B.; O'Hare, D. *Inorg. Chem.* **2005**, *44*, 3837. (e) Doran, M. B.; Cockbain, B. E.; Norquist, A. J.; O'Hare, D. *Dalton Trans.* **2004**, *22*, 3810. (f) Doran, M. B.; Norquist, A. J.; Stuart, C. L.; O'Hare, D. *Acta Crystallogr.* **2004**, *E60*, m996−m998. (g) Doran, M. B.; Norquist, A. J.; O'Hare, D. *Inorg. Chem.* **2003**, *42*, 6989.
(6) (a) Krivovichev, S. V.; Kahlenberg, V.; Tananaev, I. G.; Kaindl, R.; Mersdorf, E.; Myasoedov, B. F. *J. Am. Chem. Soc.* **2005**, *127*, 1072. (b) Krivovichev, S. V.; Kahlenberg, V.; Kaindl, R.; Mersdorf, E.; Tananaev, I. G.; Myasoedov, B. F. *Angew. Chem.* **2005**, *44*, 1134. (c) Albrecht-Schmitt, T. E. *Angew. Chem.* **2005**, *44*, 4836.

10.1021/ic701571w CCC: $37.00
Published on Web 11/03/2007

hybrid compounds some of which fall under the classification of metal-organic frameworks. This group is especially well represented by solids incorporating carboxylate linkers.[9] Luminescent and photocatalytic properties have been exploited in these materials.[9]

In this present report, we explore three new kinds of bimetallic transition metal uranyl phosphate organic−inorganic hybrids, $[Ag(4,4'\text{-bipy})]_2[(UO_2)_2H_3(PO_4)_3]$ (**AgUP-1**), $Ag(2,2'\text{-bipy})(UO_2)_2(HPO_4)(PO_4)$ (**AgUP-2**), and $[Zn(2,2'\text{-bipy})]_2[UO_2(HPO_4)_3]$ (**ZnUP-1**). These compounds display the different roles that transition metal bipyridyl complexes can play in uranyl phosphate structural chemistry. In the first compound, independent silver 4,4′-bipyridyl and uranyl phosphate networks are found, and in **AgUP-2** and **ZnUP-1** there is direct coordination by $M(2,2'\text{-bipy})^+$ (M = Ag, Zn) to uranyl phosphate sheets and chains.

Experimental Section

Syntheses. $UO_2(C_2H_3O_2)_2 \cdot 2H_2O$ (98%, Baker), UO_2 (99.8%, Alfa-Aesar), 2,2′-Bipyridyl (98%, Alfa-Aesar), AgCN (99%, Alfa-Aesar), $Zn(CN)_2$ (98%, Alfa-Aesar), H_3PO_4 (98%, Aldrich), and 4,4′-Bipyridyl (98%, Avocado), were used as received. Reactions were run in PTFE-lined Parr 4749 autoclaves with a 23 mL internal volume. Distilled and Millipore filtered water with a resistance of 18.2 MΩ·cm was used in all reactions. Standard precautions were performed for handling radioactive materials during work with $UO_2(C_2H_3O_2)_2 \cdot 2H_2O$, UO_2, and the products of the reactions. Semiquantitative EDX analyses were performed using a JEOL 7000F field emission SEM and confirmed the presence of silver, uranium, and phosphorus or zinc, uranium, and phosphorus in the crystals.

$[Ag(4,4'\text{-bipy})]_2[(UO_2)_2H_3(PO_4)_3]$ (AgUP-1). UO_2 (164 mg, 0.607 mmol), 4,4′-bipyridyl (95 mg, 0.609 mmol), AgCN (41 mg, 0.304 mmol), and H_3PO_4 (2 mL, pH = 1.3) were loaded into a 23 mL autoclave. The autoclave was sealed and heated to 160 °C in a box furnace for 3 d. The autoclave was then cooled at an average rate of 9 °C/h to 35 °C. The product consisted of yellow prisms of **AgUP-1** and an unidentified black precipitate. The product was thoroughly washed with water, then rinsed with methanol, and allowed to dry.

$Ag(2,2'\text{-bipy})(UO_2)_2(HPO_4)(PO_4)$ (AgUP-2). $UO_2(C_2H_3O_2)_2 \cdot 2H_2O$ (187 mg, 0.441 mmol), 2,2′-bipyridyl (69 mg, 0.441 mmol), $KAg(CN)_2$ (44 mg, 0.221 mmol), and H_3PO_4 (2 mL, pH = 1.37) were loaded into a 23 mL autoclave. The autoclave was sealed and heated to 180 °C in a box furnace for 3 d. The autoclave was then cooled at an average rate of 9 °C/h to 35 °C. The product consisted of yellow prisms of **AgUP-2** and a pale-yellow gel. The product was thoroughly washed with water, then rinsed with methanol, and allowed to dry.

$[Zn(2,2'\text{-bipy})]_2[UO_2(HPO_4)_3]$ (ZnUP-1). UO_2 (167 mg, 0.619 mmol), 2,2′-bipyridyl (97 mg, 0.618 mmol), $Zn(CN)_2$ (36 mg, 0.309 mmol), and H_3PO_4 (2 mL, pH = 1.3) were loaded into a 23 mL autoclave. The autoclave was sealed and heated to 180 °C in a box furnace for 3 d. The autoclave was then cooled at an average rate of 9 °C/h to 35 °C. The product consisted of yellow plates of **ZnUP-1** and a black precipitate. The product was thoroughly washed with water, then rinsed with methanol, and allowed to dry.

Crystallographic Studies. Single crystals of $[Ag(4,4'\text{-bipy})]_2[(UO_2)_2H_3(PO_4)_3]$ (**AgUP-1**), $Ag(2,2'\text{-bipy})(UO_2)_2(HPO_4)(PO_4)$ (**AgUP-2**), and $[Zn(2,2'\text{-bipy})]_2[UO_2(HPO_4)_3]$ (**ZnUP-1**) were mounted on glass fibers and optically aligned on a Bruker APEX CCD X-ray diffractometer using a digital camera. Initial intensity measurements were performed using graphite monochromated Mo Kα ($\lambda = 0.71073$ Å) radiation from a sealed tube and a monocapillary collimator. *SMART* (version 5.624) was used for preliminary determination of the cell constants and data collection control. The intensities of reflections of a sphere were collected by a combination of three sets of exposures (frames). Each set had a different ϕ angle for the crystal, and each exposure covered a range of 0.3° in ω. A total of 1800 frames were collected with an exposure time per frame of 30 s.

For these compounds, determination of integrated intensities and global refinement were performed with the Bruker *SAINT* (version 6.02) software package, using a narrow-frame integration algorithm. A numerical, face-indexed absorption correction was applied using *XPREP*.[10] The data were treated with a semiempirical absorption correction by *SADABS*.[11] The program suite *SHELXTL* (version 6.12) was used for space-group determination (*XPREP*), direct methods structure solution (*XS*), and least-squares refinement (*XL*).[10] The final refinements included anisotropic displacement parameters for all of the atoms. Secondary extinction was not noted. Some crystallographic details are given in Table 1. Additional details can be found in the Supporting Information.

Fluorescence Spectroscopy. Fluorescence emission spectra of the single crystals were acquired using a PI Acton spectrometer (SpectraPro SP 2356, Acton, NJ) that is connected to the side port of an epi-fluorescence microscope (Nikon TE-2000U, Japan). The emission signal was recorded by a back-illuminated digital CCD camera (PI Acton PIXIS:400B, Acton, NJ) operated by a PC. For all three compounds examined, the excitation was generated by a mercury lamp (X-Cite 120, EXFO, Ontario, Canada) filtered by a band-pass filter at 450−490 nm. The emission signal was filtered by a long-pass filter with a cutoff wavelength of 515 nm. The intensities of the spectra of the three compounds are not directly comparable to each other because different acquisition times and objective lenses were used.

Results and Discussion

Structural Features of $[Ag(4,4'\text{-bipy})]_2[(UO_2)_2H_3(PO_4)_3]$ (AgUP-1). The description of the structure of **AgUP-1** begins

(7) (a) Danis, J. A.; Runde, W. H.; Scott, B.; Fettinger, J.; Eichhorn, B. *Chem. Commun.* **2001**, *22*, 2378. (b) Doran, M. B.; Stuart, C. L.; Norquist, A. J.; O'Hare, D. *Chem. Mater.* **2004**, *16*, 565. (c) Locock, A. J.; Burns, P. C. *J. Solid State Chem.* **2004**, *177*, 2675.

(8) (a) Krivovichev, S. V.; Armbruster, Th.; Chernyshov, D. Y.; Burns, P. C.; Nazarchuk, E. V.; Depmeier, W. *Micropor. Mesopor. Mater.* **2005**, *78*, 225. (b) Krivovichev, S. V.; Burns, P. C.; Armbruster, Th.; Nazarchuk, E. V.; Depmeier, W. *Micropor. Mesopor. Mater.* **2005**, *78*, 217. (c) Krivovichev, S. V.; Cahill, C. L.; Nazarchuk, E. V.; Burns, P. C.; Armbruster, Th.; Depmeier, W. *Micropor. Mesopor. Mater.* **2005**, *78*, 209.

(9) (a) Frisch, M.; Cahill, C. L. *Dalton Trans.* **2006**, *39*, 4679. (b) Borkowski, L. A.; Cahill, C. L. *Cryst. Growth Des.* **2006**, *6*, 2248. (c) Borkowski, L. A.; Cahill, C. L. *Cryst. Growth Des.* **2006**, *6*, 2241. (d) Borkowski, L. A.; Cahill, C. L. *Acta Crystallogr.* **2005**, *E61*, m816−m817. (e) Frisch, M.; Cahill, C. L. *Dalton Trans.* **2005**, *8*, 1518. (f) Borkowski, L. A.; Cahill, C. L. *Acta Crystallogr.* **2004**, *E60*, m198−m200. (g) Borkowski, L. A.; Cahill, C. L. *Inorg. Chem.* **2003**, *42*, 7041. (h) Yu, Z.-T.; Liao, Z.-L.; Jiang, Y.-S.; Li, G.-H.; Chen, J.-S. *Chemistry*, **2005**, *11*, 2642. (i) Kim, J.-Y.; Norquist, A. J.; O'Hare, D. *Dalton Trans.* **2003**, *14*, 2813.

(10) Sheldrick, G. M. *SHELXTL PC, An Integrated System for Solving, Refining, and Displaying Crystal Structures from Diffraction Data*, version 6.12; Siemens Analytical X-Ray Instruments, Inc.: Madison, WI, 2001.

(11) Sheldrick, G. M. SADABS 2001, Program for Absorption Correction Using SMART CCD Based on the Method of Blessing; Blessing, R. H., Ed.; *Acta Crystallogr.* **1995**, *A51*, 33.

Table 1. Crystallographic Data for $[Ag(4,4'\text{-bipy})]_2[(UO_2)_2H_3(PO_4)_3]$ (**AgUP-1**), $Ag(2,2'\text{-bipy})(UO_2)_2(HPO_4)(PO_4)$ (**AgUP-2**), and $[Zn(2,2'\text{-bipy})]_2[UO_2(HPO_4)_3]$ (**ZnUP-1**)

compound	AgUP-1	AgUP-2	ZnUP-1
formula mass	1356.10	995.06	1001.07
color and habit	Yellow, block	Yellow, needle	Yellow, plate
space group	$P\bar{1}$	$P\bar{1}$	$P\bar{1}$
a (Å)	7.0342(5)	9.3642(18)	10.9496(8)
b (Å)	10.6929(7)	9.8038(19)	11.4702(8)
c (Å)	11.1301(8)	10.488(2)	12.9805(9)
α (deg)	93.682(1)	100.350(3)	67.222(1)
β (deg)	106.908(1)	98.449(3)	86.708(1)
γ (deg)	107.031(1)	93.135(3)	66.378(1)
V (Å^3)	755.57(9)	933.6(3)	1367.94(17)
Z	1	2	2
T (K)	193	193	193
λ (Å)	0.71073	0.71073	0.71073
maximum 2θ (deg)	28.30	28.47	28.36
ρ_{calcd} (g cm^{-3})	2.974	3.536	2.423
μ(Mo $K\alpha$) (cm^{-1})	122.01	185.80	78.99
$R(F)$ for $F_o^2 > 2\sigma(F_o^2)$[a]	0.0382	0.0291	0.0317
$R_w(F_o^2)$[b]	0.0967	0.0871	0.0751

[a] $R(F) = \sum||F_o| - |F_c||/\sum|F_o|$. [b] $R_w(F_o^2) = [\sum[w(F_o^2 - F_c^2)^2]/\sum wF_o^4]^{1/2}$.

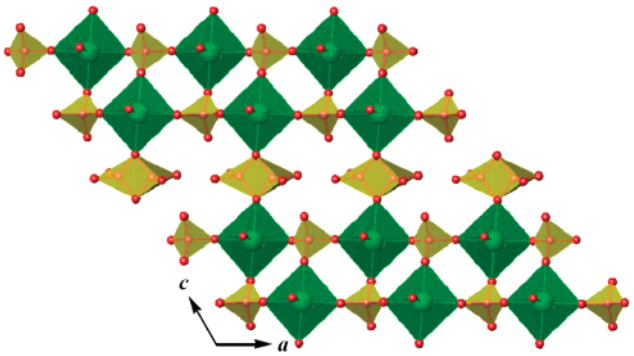

Figure 1. View of the $^2_\infty[(UO_2)_2H_3(PO_4)_3]^{2-}$ layers that extend in the [ac] plane in the structure of $[Ag(4,4'\text{-bipy})]_2[(UO_2)_2H_3(PO_4)_3]$ (**AgUP-1**). UO_6 tetragonal bipyramids are shown in green, and phosphate tetrahedra are shown in yellow.

with the presence of a classical uranyl, UO_2^{2+}, unit that is nearly linear with a O(9)−U1−O(8) bond angle of 179.3(2)° and normal U═O bond distances of 1.788(5) and 1.791(5) Å. Four oxygen atoms are found approximately perpendicular to the uranyl axis, creating an environment that is best described as a tetragonal bipyramid. These donor atoms belong to phosphate anions found within the structure, and the U−O bond distances range from 2.261(5) to 2.313(6) Å. Using these distances, a bond-valence sum[12,13] of 6.1 was arrived at for U(1), which is consistent with this compound containing uranium(VI).[1]

The phosphate anions bridge uranyl cations to create ribbons that extend in the a axis direction. These ribbons are similar to those found in compounds and minerals with the autunite-layered topology.[2] The ribbons are in turn linked to one another through phosphate anions to create $^2_\infty[(UO_2)_2H_3(PO_4)_3]^{2-}$ layers in the [ac] plane that are shown in Figure 1. This is a new anionic sheet topology for uranyl compounds that is related to the sheets found in $(NH_4)_2[(UO_2)_2(CrO_4)_3(H_2O)_2](H_2O)_4$[14] and $K_2[(UO_2)_2(CrO_4)_3(H_2O)_2](H_2O)_4$[15] except that these latter compounds contain

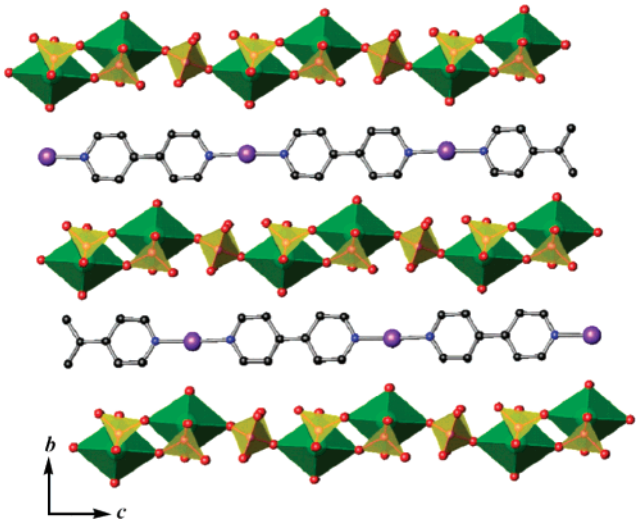

Figure 2. Depiction of the separation of uranyl phosphate layers are from one another by $^1_\infty[Ag(4,4'\text{-bipy})]^+$ chains formed from two-coordinate Ag^+ bridged by 4,4′-bipy in $[Ag(4,4'\text{-bipy})]_2[(UO_2)_2H_3(PO_4)_3]$ (**AgUP-1**). UO_6 tetragonal bipyramids are shown in green, phosphate tetrahedra are shown in yellow, and Ag^+ cations are shown in purple.

UO_7 pentagonal bipyramids instead of UO_6 tetragonal bipyramids. One of the phosphate anions is disordered with two different, but equally occupied, orientations being present. The P−O distances can be distinguished from the P−OH distances on the basis of the bond length and whether or not they are terminal or bridging oxygen atoms. For P(1), the longest P−O bond distance of 1.551(6) Å also corresponds to a terminal oxygen atom, and this therefore is likely to be the site of protonation. For P(2), there are two such terminal oxygen atoms; however, owing to the disorder of this anion, the P−O bond distances are irregular, and bond distance analysis is not possible. Small channels through the sheets are formed where there are appropriate distances between protonated phosphate anions to create hydrogen bonding interactions. These interactions might be the source of the novel sheet topology observed for **AgUP-1**.

The uranyl phosphate layers are separated from one another by $^1_\infty[Ag(4,4'\text{-bipy})]^+$ chains formed from two-coordinate Ag^+ cations bridged by 4,4′-bipy, as is shown in Figure 2. The Ag−N distances of 2.100(6) and 2.123(6) Å are normal. The N(1)−Ag(1)−N(2) angle is nearly linear with an angle of 176.3(2)°. This is apparently the first example of uranyl-containing layers being separated by a coordination polymer. Selected bond distances and angles are given in Table 2.

Structural Features of $Ag(2,2'\text{-bipy})(UO_2)_2(HPO_4)(PO_4)$ (AgUP-2). Whereas the structure of **AgUP-2** also contains 2D uranyl phosphate layers, Ag^+, and bipy ligands, its structure is substantially different from that of **AgUP-1** for a number of reasons. Foremost among these is that 4,4′-bipy has been exchanged for 2,2′-bipy, and this prevents the formation of a $Ag(bipy)^+$ extended substructure, owing to the chelating nature of 2,2′-bipy. Additionally, the funda-

(12) Brown, I. D.; Altermatt, D. *Acta Crystallogr.* **1985**, *B41*, 244.
(13) Brese, N. E.; O'Keeffe, M. *Acta Crystallogr.* **1991**, *B47*, 192.
(14) Mikhailov, Yu. N.; Gorbunova, Yu. E.; Serezhkina, L. B.; Serezhkin, V. N. *Russ. J. Inorg. Chem.* **1997**, *42*, 652.
(15) Krivovichev, S. V.; Burns, P. C. *Z. Kristallogr.* **2003**, *218*, 725.

Table 2. Selected Bond Distances (Angstroms) and Angles (Degrees) for $[Ag(4,4'\text{-bipy})]_2[(UO_2)_2H_3(PO_4)_3]$ (**AgUP-1**)[a]

distances (Å)			
U(1)−O(3)	2.313(6)	P(1)−O(1)	1.541(14)
U(1)−O(5)#2	2.279(5)	P(1)−O(2)	1.571(12)
U(1)−O(6)#1	2.261(5)	P(1)−O(3)	1.656(7)
U(1)−O(7)	2.265(5)	P(1)−O(3)#3	1.586(7)
U(1)−O(8)	1.788(5)	P(2)−O(4)	1.551(6)
U(1)−O(9)	1.791(5)	P(2)−O(5)	1.527(5)
Ag(1)−N(1)	2.100(6)	P(2)−O(6)	1.534(5)
Ag(1)−N(2)	2.123(6)	P(2)−O(7)	1.535(6)
	Angles (deg)		
O(8)−U(1)−O(9)	179.3(2)	N(1)−Ag(1)−N(2)	176.3(2)

[a] Symmetry transformations used to generate equivalent atoms: #1 $-x+1, -y, -z$; #2 $x-1, y, z$; #3 $-x, -y, -z-1$.

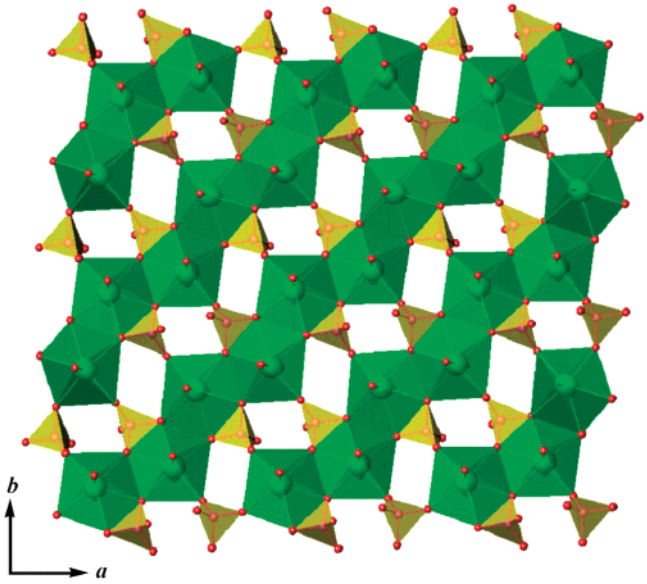

Figure 3. Illustration of the $^2_\infty[(UO_2)_2(HPO_4)(PO_4)]^{1-}$ sheets with the β-uranophane topology that extend in the [*ab*] plane in the structure of $Ag(2,2'\text{-bipy})(UO_2)_2(HPO_4)(PO_4)$ (**AgUP-2**). UO_7 pentagonal bipyramids are shown in green, and phosphate tetrahedra are shown in yellow.

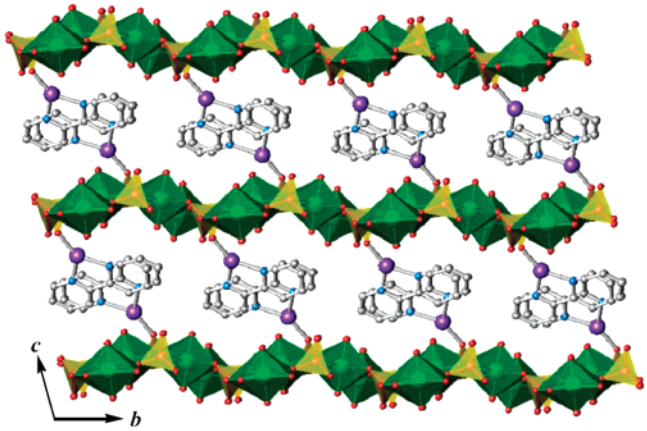

Figure 4. View of the decoration of $^2_\infty[(UO_2)_2(HPO_4)(PO_4)]^{1-}$ sheets by $[Ag(2,2'\text{-bipy})]^+$ moieties in $Ag(2,2'\text{-bipy})(UO_2)_2(HPO_4)(PO_4)$ (**AgUP-2**). UO_7 pentagonal bipyramids are shown in green, phosphate tetrahedra are shown in yellow, and Ag^+ cations are shown in purple.

mental uranyl-containing building units found here are the more common UO_7 pentagonal bipyramids. There are two crystallographically unique building units with U=O bond distances being slightly shorter than normal at 1.737(5) to 1.766(5) Å. Both units are also nearly linear with bond angles

Table 3. Selected Bond Distances (Angstroms) and Angles (Degrees) for $Ag(2,2'\text{-bipy})(UO_2)_2(HPO_4)(PO_4)$ (**AgUP-2**)[a]

distances (Å)			
U(1)−O(2)#1	2.282(4)	U(2)−O(11)	1.762(5)
U(1)−O(4)	2.369(4)	U(2)−O(12)	1.737(5)
U(1)−O(5)	2.497(4)	Ag(1)−N(1)	2.100(6)
U(1)−O(5)#2	2.388(4)	Ag(1)−N(2)	2.123(6)
U(1)−O(8)	2.555(4)	P(1)−O(1)	1.518(5)
U(1)−O(9)	1.766(5)	P(1)−O(2)	1.500(4)
U(1)−O(10)	1.753(5)	P(1)−O(3)	1.547(4)
U(2)−O(3)	2.454(4)	P(1)−O(4)	1.549(4)
U(2)−O(3)#4	2.373(4)	P(2)−O(5)	1.537(4)
U(2)−O(4)	2.526(4)	P(2)−O(6)	1.561(5)
U(2)−O(7)#3	2.311(4)	P(2)−O(7)	1.492(4)
U(2)−O(8)	2.385(4)	P(2)−O(8)	1.519(4)
	Angles (deg)		
O(1)−Ag(1)−N(2)	148.2(2)	O(1)−Ag(1)−N(1)	137.2(2)
N(2)−Ag(1)−N(1)	73.1(2)		

[a] Symmetry transformations used to generate equivalent atoms: #1 $-x+2, -y+1, -z+1$; #2 $-x+1, -y+1, -z+1$; #3 $-x+1, -y, -z+1$; #4 $-x+2, -y, -z+1$.

Table 4. Selected Bond Distances (Angstroms) and Angles (Degrees) for $[Zn(2,2'\text{-bipy})]_2[UO_2(HPO_4)_3]$ (**ZnUP-1**)[a]

distances (Å)			
U(1)−O(2)	2.322(3)	Zn(2)−O(6)#2	1.959(3)
U(1)−O(7)	2.484(3)	Zn(2)−O(8)	2.036(3)
U(1)−O(8)	2.472(3)	P(1)−O(1)	1.576(3)
U(1)−O(11)	2.294(3)	P(1)−O(2)	1.531(3)
U(1)−O(12)#1	2.306(3)	P(1)−O(3)	1.520(3)
U(1)−O(13)	1.776(3)	P(1)−O(4)	1.507(3)
U(1)−O(14)	1.797(3)	P(2)−O(5)	1.579(3)
Zn(1)−N(1)	2.102(4)	P(2)−O(6)	1.495(3)
Zn(1)−N(2)	2.061(4)	P(2)−O(7)	1.521(3)
Zn(1)−O(4)	1.929(3)	P(2)−O(8)	1.542(3)
Zn(1)−O(10)	1.946(3)	P(3)−O(9)	1.570(3)
Zn(2)−N(3)	2.130(4)	P(3)−O(10)	1.536(3)
Zn(2)−N(4)	2.085(4)	P(3)−O(11)	1.525(3)
Zn(2)−O(3)	2.035(3)	P(3)−O(12)	1.517(3)
	Angles (deg)		
N(2)−Zn(1)−N(1)	79.11(16)	N(4)−Zn(2)−N(3)	77.49(16)
O(4)−Zn(1)−O(10)	113.87(13)	O(3)−Zn(2)−O(8)	90.08(13)

[a] Symmetry transformations used to generate equivalent atoms: #1 $-x+1, -y, -z+1$; #2 $-x+1, -y+1, -z$.

of 178.0(2) and 179.4(2)° for U(1) and U(2), respectively. The five equatorial distances range from 2.282(4) to 2.555(4) Å for U(1) and from 2.311(4) to 2.526(4) Å for U(2). This allows for the determination of the bond-valence sums[12,13] for U(1) and U(2) of 5.9 and 6.0, respectively.[1] The UO_7 units share two opposite edges, to create 1D chains that are joined to one another by phosphate and hydrogen phosphate anions to yield $^2_\infty[(UO_2)_2(HPO_4)(PO_4)]^{1-}$ sheets with the β-uranophane topology that extend in the [*ab*] plane as is shown in Figure 3.[2]

Fortunately there is no disorder in the structure of **AgUP-2**, and the longest terminal P(2)−O bond distance of 1.561(5) Å likely corresponds to the site of protonation. P(1) also possesses an oxo atom that is directed between the layers, much like the P(2)−OH group. However, here the O(1) atom bridges between P(1) and Ag(1). Therefore, there is direct coordination by the Ag^+ centers to the $^2_\infty[(UO_2)_2(HPO_4)(PO_4)]^{1-}$ sheets, making **AgUP-2** fundamentally different in construction from **AgUP-1**. The coordination sphere of the

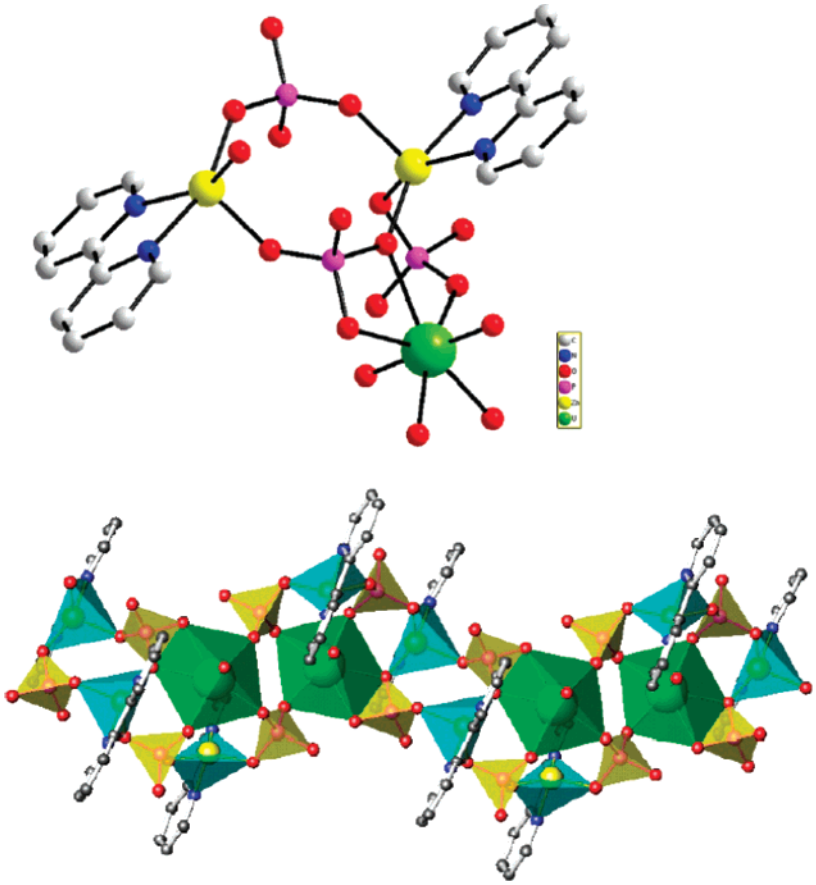

Figure 5. Depiction of the basic repeating units for $[Zn(2,2'\text{-bipy})]_2[UO_2(HPO_4)_3]$ (**ZnUP-1**). UO_7 pentagonal bipyramids are shown in green, phosphate tetrahedra are shown in yellow, and Zn^{2+} cations are shown in yellow (inside of the blue polyhedra).

Ag^+ center is completed by one chelating 2,2′-bipy ligand, making the silver atom three-coordinate with a distorted trigonal-planar environment with Ag−O and Ag−N (×2) distances of 2.185(4), 2.259(6), and 2.318(7) Å. The $[Ag(2,2'\text{-bipy})]^+$ moieties can be thought of as decorating the top and bottom of the uranyl phosphate layers in **AgUP-2**, as is depicted in Figure 4. Selected bond distances and angles are given in Table 3.

Structural Features of $[Zn(2,2'\text{-bipy})]_2[UO_2(HPO_4)_3]$ (ZnUP-1). The structure of **ZnUP-1** is the most complex of the three compounds. The metal centers are found as $[UO_7]$ pentagonal bipyramids, $[ZnN_2O_2]$ highly distorted tetrahedra, and $[ZnN_2O_3]$ distorted trigonal bipyramids. The uranyl moieties are bound by both bridging and bridging/chelating phosphate anions. The phosphate groups further ligate two different zinc centers. Zn(1) is bound by phosphate groups to the periphery of the chains, whereas Zn(2), found as $[ZnN_2O_3]$ units, is located within the chain and is an integral feature of chain propagation. The basic repeating unit for **ZnUP-1** is shown in Figure 5. The bound 2,2′-bipy molecules lie perpendicular to the chains and are loosely π-stacked with 2,2′-bipy molecules from neighboring chains with a stacking distance of approximately 3.48 Å. A view of packing of the chains is shown in Figure 6.

The UO_7 pentagonal bipyramid is composed of a central uranyl, UO_2^{2+}, cation with normal U═O bond distances of 1.776(3) and 1.797(3) Å. The five equatorial U−O distances

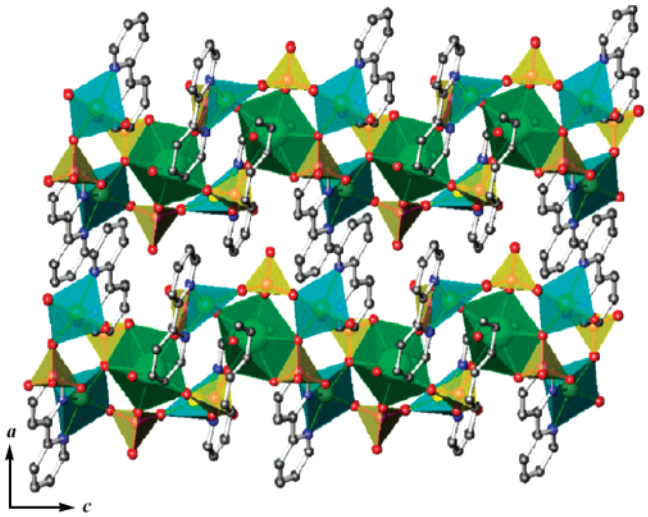

Figure 6. View of packing of the chains in $[Zn(2,2'\text{-bipy})]_2[UO_2(HPO_4)_3]$ (**ZnUP-1**). UO_7 pentagonal bipyramids are shown in green, phosphate tetrahedra are shown in yellow, and Zn^{2+} cations are shown in yellow (inside of the blue polyhedra).

range from 2.294(3) to 2.484(3) Å. Taken together, these distances result in a bond-valence sum of 6.0.[1,12,13] The Zn(1) atom is bound by one 2,2′-bipy molecule and two phosphate anions to create $[ZnN_2O_2]$ highly distorted tetrahedra. Zn(1)−N bond distances are 2.061(4) and 2.102(4) Å. The Zn(1)−O distances are 1.929(3) and 1.946(3) Å. Zn-

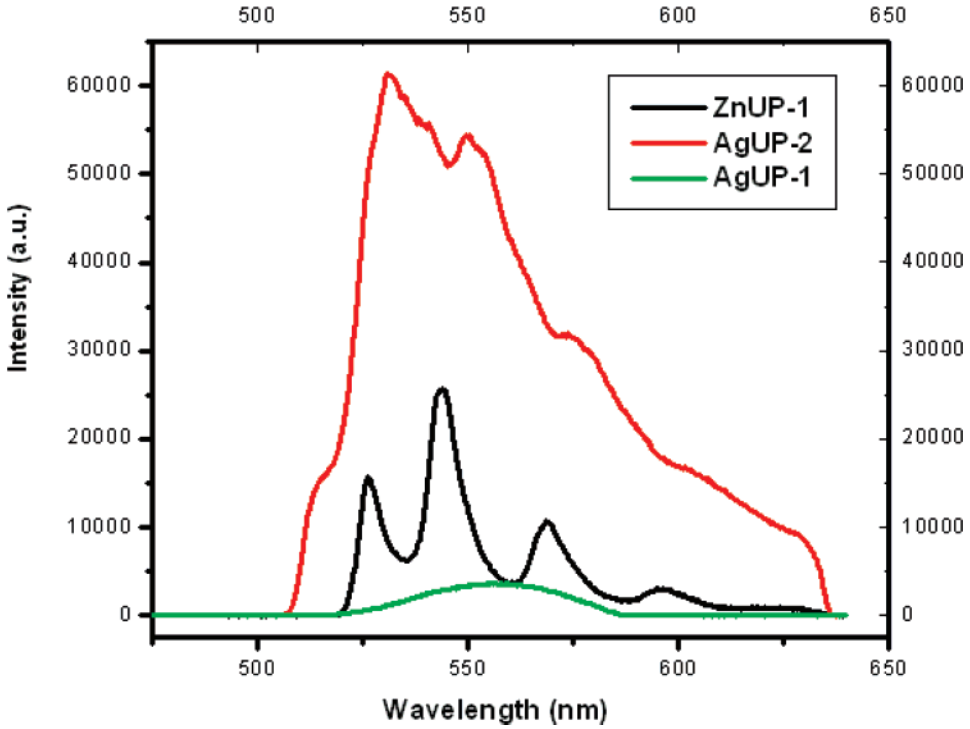

Figure 7. Fluorescence emission spectra from $[Ag(4,4'\text{-bipy})]_2[(UO_2)_2H_3(PO_4)_3]$ (**AgUP-1**), $Ag(2,2'\text{-bipy})(UO_2)_2(HPO_4)(PO_4)$ (**AgUP-2**), and $[Zn(2,2'\text{-bipy})]_2[UO_2(HPO_4)_3]$ **(ZnUP-1)**. See Experimental section for more details.

(2) is found as $[ZnN_2O_3]$ distorted trigonal bipyramids, where the Zn(2) center is bonded to one 2,2′-bipy molecule and three phosphate anions. Zn(2)−N bond distances are 2.085(4) and 2.130(4) Å; whereas the Zn(2)−O distances are slightly shorter and range from 1.959(3) to 2.036(3) Å. There are three crystallographically unique phosphate anions. Each of these anions has three short P−O bonds, which average 1.521(3) Å for the three anions, and one long P−O bond of 1.575(3) Å. The length of the long bond is consistent with this oxygen atom being protonated, which also allows the compound to achieve charge neutrality. Selected bond distances and angles for this compound can be found in Table 4.

Fluorescence Spectroscopy. The emission of green light from uranyl compounds excited by long-wavelength UV light has been known for centuries. Fluorescence from uranyl compounds can be identified from the vibronic fine-structure characteristic of the UO_2^{2+} moiety.[16,17] Emission from uranyl-containing networks is complex and easily influenced by subtle changes in bonding, as indicated by Grohol and Clearfield's report on the luminescent properties of two closely related uranyl phosphonates, $[UO_2(HO_3PC_6H_5)_2(H_2O)]_2\cdot 8H_2O$ and $UO_2(HO_3PC_6H_5)_2(H_2O)\cdot 2H_2O$, whose structural differences are based largely on conformational changes in the phosphonate anions.[18] More recently it has been demonstrated uranyl compounds containing aromatic organic moieties can exhibit the antenna effect, yielding enhanced emission by the uranyl cations.[9a,19] The fluorescence spectra of $[Ag(4,4'\text{-bipy})]_2[(UO_2)_2H_3(PO_4)_3]$ (**AgUP-1**), $Ag(2,2'\text{-bipy})(UO_2)_2(HPO_4)(PO_4)$ (**AgUP-2**), and $[Zn(2,2'\text{-bipy})]_2[UO_2(HPO_4)_3]$ **(ZnUP-1)** are shown in Figure 7. As can be discerned from these data, these compounds exhibit substantial differences in their emission properties. First, whereas the fluorescence of **AgUP-1** is observed, all of the fine structure is lost. Second, whereas the emission from **AgUP-2** is quite strong, again much of the fine structure is lost. Finally, the emission from **ZnUP-1** is classic, with strong emission and clearly resolved fine structure being present.

Conclusions

In this report, we have demonstrated new methods for constructing inorganic−organic hybrid uranyl phosphates. In **AgUP-1**, there are independent $^1_\infty[Ag(4,4'\text{-bipy})]^+$ cationic and $^2_\infty[(UO_2)_2H_3(PO_4)_3]^{2-}$ anionic networks. In contrast, by replacing the 4,4′-bipy with 2,2′-bipy, cationic $[Ag(2,2'\text{-bipy})]^+$ moieties are obtained that are directly coordinated by phosphate anions in the $^2_\infty[(UO_2)_2(HPO_4)(PO_4)]^{1-}$ layers, to yield decorated sheetsin **AgUP-2**. **ZnUP-1** shows yet another way that transition metal 2,2′-bipy complexes can be incorporated into uranyl phosphate networks in that there is decoration of uranyl phosphate chains as well as direct incorporation of the Zn^{2+} cations into the chains. Each of these compounds exhibits different fluorescence properties, indicating that the transition metal bipy moieties affect the emission from the uranyl cations.

(16) Carnall, W. T.; Crosswhite, H. M. In *The Chemistry of the Actinide Elements*; Katz, J. J., Seaborg, G. T., Morss, J. R., Eds; Chapman and Hall: London, 1986; Chapter 16.
(17) Denning, R. G.; Norris, J. O. W.; Short, I. G.; Snellgrove, T. R.; Woodwark, D. R. *Lanthanide and Actinide Chemistry and Spectroscopy*; ACS Symp. Ser. no. 131; Edelstein, N. M., Ed.; American Chemical Society: Washington, DC, 1980, Chapter 15.
(18) Grohol, D.; Clearfield, A. *J. Am. Chem. Soc.* **1997**, *119*, 4662.
(19) Almond, P. M.; Talley, C. E.; Bean, A. C.; Peper, S. M.; Albrecht-Schmitt, T. E. *J. Solid State Chem.* **2000**, *154*, 635.

Acknowledgment. This work was supported by the Chemical Sciences, Geosciences and Biosciences Division, Office of Basic Energy Sciences, Office of Science, Heavy Elements Program, U.S. Department of Energy under Grant DE-FG02-01ER15187.

Supporting Information Available: X-ray crystallographic files in CIF format for $[Ag(4,4'\text{-bipy})]_2[(UO_2)_2H_3(PO_4)_3]$ (**AgUP-1**), $Ag(2,2'\text{-bipy})(UO_2)_2(HPO_4)(PO_4)$ (**AgUP-2**), and $[Zn(2,2'\text{-bipy})]_2[UO_2(HPO_4)_3]$ **(ZnUP-1)**. This material is available free of charge via the Internet at http://pubs.acs.org.

IC701571W